Photoexcitation in Cu(I) and Re(I) Complexes Containing Substituted Dipyrido[3,2-*a*:2′,3′-*c*]phenazine: A Spectroscopic and Density Functional Theoretical Study

Penny J. Walsh, Keith C. Gordon,* Natasha J. Lundin, and Allan G. Blackman

Department of Chemistry, University of Otago, Dunedin, New Zealand

Received: February 27, 2005; In Final Form: May 3, 2005

Copper(I) and rhenium(I) complexes $[Cu(PPh_3)_2(dppz\text{-}11\text{-}COOEt)]BF_4$, $[Cu(PPh_3)_2(dppz\text{-}11\text{-}Br)]BF_4$, $[Re(CO)_3Cl(dppz\text{-}11\text{-}COOEt)]$ and $[Re(CO)_3Cl(dppz\text{-}11\text{-}Br)]$ (dppz-11-COOEt = dipyrido-[3,2a:2′,3′c]phenazine-11-carboxylic ethyl ester, dppz-11-Br = 11-bromo-dipyrido[3,2a:2′,3′c]-phenazine) have been studied using Raman, resonance Raman, and transient resonance Raman (TR^2) spectroscopy, in conjunction with computational chemistry. DFT (B3LYP) frequency calculations with a 6-31G(d) basis set for the ligands and copper(I) centers and an effective core potential (LANL2DZ) for rhenium in the rhenium(I) complexes show close agreement with the experimental nonresonance Raman spectra. Modes that are phenazine-based, phenanthroline-based, and delocalized across the entire ligand structure were identified. The nature of the absorbing chromophores at 356 nm for ligands and complexes was established using resonance Raman spectroscopy in concert with vibrational assignments from calculations. This analysis reveals that the dominant chromophore for the complexes measured at 356 nm is ligand-centered (LC), except for $[Re(CO)_3Cl(dppz\text{-}11\text{-}Br)]$, which appears to have additional chromophores at this wavelength. Calculations on the reduced complexes, undertaken to model the metal-to-ligand charge transfer (MLCT) excited state, show that the reducing electron occupies a ligand MO that is delocalized across the ligand structure. Resonance Raman spectra (λ_{exc} = 514.5 nm) of the reduced rhenium complexes show a similar spectral pattern to that observed in $[Re(CO)_3Cl(dppz)]^{\cdot -}$; the measured bands are therefore attributed to ligand radical anion modes. These bands lie at 1583−1593 cm^{-1} for $[Re(CO)_3Cl(dppz\text{-}11\text{-}COOEt)]$ and 1611 cm^{-1} for $[Re(CO)_3Cl(dppz\text{-}11\text{-}Br)]$. The thermally equilibrated excited states are examined using nanosecond-TR^2 spectroscopy (λ_{exc} = 354.7 nm). The TR^2 spectra of the ligands provide spectral signatures for the ^{3}LC state. A band at 1382 cm^{-1} is identified as a marker for the ^{3}LC states of both ligands. TR^2 spectra of the copper and rhenium complexes of dppz-11-Br show this ^{3}LC band, but it is not prominent in the spectra of $[Cu(PPh_3)_2(dppz\text{-}11\text{-}COOEt)]^+$ and $[Re(CO)_3Cl(dppz\text{-}11\text{-}COOEt)]$. Calculations suggest that the lowest triplet states of both of the rhenium(I) complexes and $[Cu(PPh_3)_2(dppz\text{-}11\text{-}Br)]^+$ are metal-to-ligand charge transfer in nature, but the lowest triplet state of $[Cu(PPh_3)_2(dppz\text{-}11\text{-}COOEt)]^+$ appears to be LC in character.

I. Introduction

Complexes containing dipyrido[3,2-*a*:2′,3′-*c*]phenazine (dppz) and its derivatives have been widely studied because of their interesting interactions with DNA.[1−3] Intercalation of dppz complexes with DNA can result in an increase in the complexes' emission quantum yield. The reasons for this so-called "light switch effect" are the presence of a group of excited states that lie at similar energy yet possess radically different electronic properties. A series of detailed photophysical and theoretical studies[4−7] suggests that the excited states of rhenium(I) and ruthenium(II) complexes containing dppz involve the presence of two low-lying triplet metal-to-ligand charge transfer (^{3}MLCT) states and a triplet ligand-centered (^{3}LC) state.

The dppz ligands may be described as having a phenanthroline (phen) portion (Figure 1, A, B, and C rings) and a phenazine (phz) portion (Figure 1, C, D, and E rings). The two ^{3}MLCT states consist of an excited electron which occupies a ligand molecular orbital (MO) that is phen- and phz-based, respectively. These ^{3}MLCT states have been shown to have very different emission quantum yields.[8] The M→phen state is emissive, but the M→phz state is not, and has been termed a dark state for this reason.

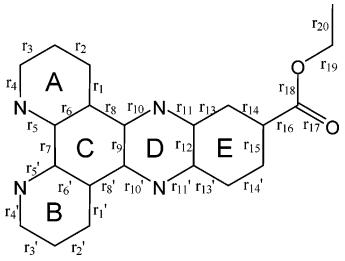

Figure 1. Schematic of dppz-11-COOEt (**1**) showing bond and ring labels.

The rationale for the "light switch effect" is the energetics of these states. The previous view held that the dark (phz) excited state is higher in energy,[6] but in protic environments hydrogen bonding causes stabilization of this state. Hence the luminescence is quenched, and nonradiative decay is from the dark state. Brennaman et al.[8] showed that the M→phen state is entropically favored over the enthalpically favored M→phz "dark" state. This is because the dark state involves a more significant reorganization of solvent due to its greater charge

* Corresponding author. E-mail: kgordon@alkali.otago.ac.nz.

10.1021/jp051009w CCC: $30.25
Published on Web 06/14/2005

separation. The emission quantum yield of $[Ru(phen)_2(dppz)]^{2+}$ is temperature-dependent; as the temperature is lowered, the lower enthalpy dark state is preferentially populated and the emission decreases.

The interplay between these close lying states is a sensitive function of metal ion,[9] solvent,[9−11] and substitutent.[12] This can allow for tuning of various electrooptical properties.

Understanding of the processes which occur in dppz complexes is vital to the development of rationally designed complexes for applications in photoelectrochemical cells[13] and therapeutic drugs.[14,15] Complexes of dppz derivatives are also useful as components in organic light emitting devices (OLEDs) because their emission color is largely red-shifted from their absorption wavelength.[16] This allows red emission from complexes which absorb little in the visible region.

Computational chemistry can offer some insight into the spectroscopic properties and the processes involved in excitation and subsequent decay of the excited states. Pourtois et al.[17] used a variety of computational methods to examine the nature of the excited states in $[Ru(phen)_2(dppz)]^{2+}$. They used the semiempirical method AM1 to model the geometry of various polypyridyl ligands, followed by HF/INDO modeling of Ru(II) polypyridyl complexes. Excited states were modeled with AM1/CAS-CI treatments (ligands) and SCI/INDO (Ru(II) complexes). The Franck−Condon (FC) gas-phase triplet excited-state energies for $[Ru(phen)_2(dppz)]^{2+}$ were also modeled with TDDFT to check the relative energetic ordering of excited states. The authors concluded from their calculations that the lowest excited state for $[Ru(phen)_2(dppz)]^{2+}$ is a triplet intraligand (^{3}-LC) state.

Further studies, including TDDFT of the singlet states of $[Ru(phen)_2(dppz)]^{2+}$, were conducted by Fantacci et al. in order to study the UV/visible absorption profile of this complex.[18] Importantly, they found that the inclusion of solvation effects in calculations on Ru-dppz systems raises the absolute orbital energies by about 4 eV and changes the energy ordering of the MOs. In particular, the HOMOs become t_{2g}(Ru) in solution, while in vacuo the HOMO is π(dppz). Solvent effects become important in TDDFT calculations on *fac*-$[Re(CO)_3(py)(dppz)]^+$, affecting the relative energetic ordering of calculated triplet states.[19] A recent TDDFT/B3LYP study by Batista et al.[20] showed that solvent effects are crucial in considering the low-lying excited states of the $[Ru(bpy)_2(dppz)]^{2+}$ complex and supported the finding by Pourtois et al. that the lowest excited state of $[Ru(bpy)_2(dppz)]^{2+}$ is a $^3\pi-\pi^*$ state similar to that of $[Ru(phen)_2(dppz)]^{2+}$.

Transient vibrational spectroscopy may be used to establish the nature of excited states in polypyridyl complexes.[21] Transient Raman spectroscopy has been used with considerable success in heteroleptic complexes to determine the terminating ligand for MLCT excited states. However, it is much more difficult to use vibrational data to assign terminating MOs on a single ligand, which may be important for the dppz systems. A time-resolved IR study was undertaken on *fac*-[Re(CO)$_3$(Cl)(dppz-11-COOEt)] to monitor the changes upon excitation in the four ν(CO) modes present in this complex; the authors identified a dπ(Re) → π^*(phz) ^{3}MLCT state which was not emissive in CH_3CN at room temperature as it had a lifetime of only 220 ps.[22]

In this report, we have used resonance Raman and transient resonance Raman spectroscopy, in concert with DFT calculations, to probe the ground state, FC state and thermally equilibrated excited (THEXI)[23] states in copper(I) and rhenium(I) dppz-based complexes. We have used DFT calculations to predict the structure and vibrational spectra of the ground states of the compounds, as well as the reduced states and the lowest triplet or THEXI states. The latter calculations have been found to be useful models for the excited states of metal polypyridyl complexes.[9,19,24,25] Adding an electron to the compound may model the effects of MLCT excitation. In an MLCT state, the metal center is oxidized and the ligand reduced, while in the reduced complex, the additional electron occupies a molecular orbital on the polypyridyl ligand. In a triplet state calculation, the electron configuration is that of the lowest-energy excited state. It has previously been shown that calculations can predict the structure and vibrational spectra of the complexes studied in this work.[25] The reliability of calculated parameters may be tested by comparison with observables such as the vibrational spectra. If a good correlation is achieved between theory and experiment, the calculation gives insight into the electronic properties of the complexes.

II. Experimental Section

The syntheses of dppz-11-COOEt (1) (Figure 1) and dppz-11-Br (**2**) have been reported elsewhere.[25] Complexation to copper(I) and rhenium(I) centers produced the complexes $[Cu(PPh_3)_2$(dppz-11-COOEt)$]BF_4$ ($[Cu(PPh_3)_2$(**1**)$]^+$), $[Cu(PPh_3)_2$(dppz-11-Br)$]BF_4$ ($[Cu(PPh_3)_2$(**2**)$]^+$), $[Re(CO)_3Cl$(dppz-11-COOEt)] ($[Re(CO)_3Cl$(**1**)]), and $[Re(CO)_3Cl$(dppz-11-Br)] ($[Re(CO)_3Cl$(**2**)]).[25]

The Gaussian 03W package[26] was used to perform ground state, reduced state, and lowest triplet state calculations for **1**, **2** and their complexes with $[Cu(PH_3)_2]^+$ and $[Re(CO)_3Cl]$. For the copper(I) complexes, the triphenylphosphine ligands were represented by PH_3 groups to reduce the number of degrees of freedom.[27] The geometry optimizations, vibrational frequencies and their IR and Raman intensities were calculated using DFT (B3LYP/6-31G(d)). Rhenium centers were represented using the effective core potential LANL2DZ. Illustration of vibrational modes was achieved using the Molden package.[28]

The optimized structure was used to calculate vibrational frequencies. Importantly, none of the frequency calculations generated negative frequencies; this is consistent with an energy minimum for the optimized geometry. Frequencies were scaled using the frequency scaling factor 0.975, as this provided the lowest mean absolute deviation between experimental and calculated band frequencies in the 1000−1700 cm^{-1} region, for the series of compounds studied.

FT-Raman spectra were collected on powder samples using a Bruker IFS-55 interferometer with an FRA/106S attachment. The excitation source was an Nd:YAG laser with an excitation wavelength of 1064 nm. A Ge diode (D424) operating at room temperature was used to detect Raman photons. All spectra were taken with a laser power of 105 mW at the sample and a resolution of 4 cm^{-1}, using 16−64 scans.

Resonance Raman spectra, generated with continuous wave excitation, were obtained using a krypton-ion laser (Coherent Innova I-302). Plasma emission lines were removed from the exciting beam using band-pass filters or a wavelength specific holographic laser band-pass filter (Kaiser Optical Systems Inc.). Typically the laser output was adjusted to give 25 mW at the sample. The sample was held in a spinning NMR tube or optically transparent thin layer electrode (OTTLE) cell. The incident beam and the collection lens were arranged in a 135° backscattering geometry to reduce Raman intensity reduction by self-absorption. An aperture-matched lens was used to focus scattered light through a narrow band line-rejection (notch) filter (Kaiser Optical Systems) and a quartz wedge (Spex) and onto

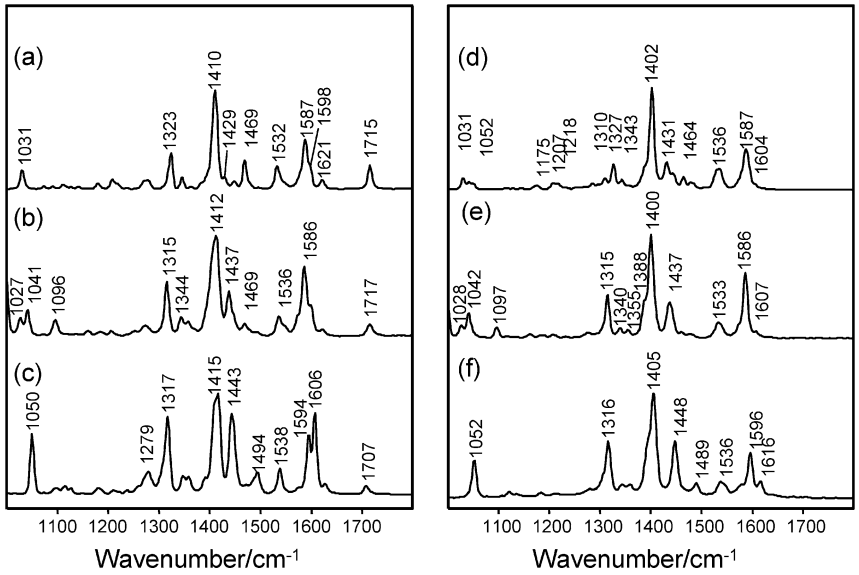

Figure 2. Solid-state FT-Raman spectra ($\lambda_{exc} = 1064$ nm) of (a) **1**, (b) $[Cu(PPh_3)_2(\mathbf{1})]^+$, (c) *fac*-$[Re(CO)_3Cl(\mathbf{1})]$, (d) **2**, (e) $[Cu(PPh_3)_2(\mathbf{2})]^+$, and (f) *fac*-$[Re(CO)_3Cl(\mathbf{2})]$.

the 100 μm entrance slit of a spectrograph (Acton Research SpectraPro 500i). The collected light was dispersed in the horizontal plane by a 1200 grooves/mm ruled diffraction grating (blaze wavelength 500 nm) and detected by a liquid nitrogen cooled back-illuminated Spec-10:100B CCD controlled by a ST-133 controller and WinSpec/32 (version 2.5.8.1) software (Roper Scientific, Princeton Instruments).

The Raman spectra of reduced species were measured using an OTTLE cell with a platinum grid as the working electrode.[12] Spectra were recorded in acetonitrile at 0.5 mM concentration for *fac*-$[Re(CO)_3Cl(\mathbf{2})]$ and a saturated solution for *fac*-$[Re(CO)_3Cl(\mathbf{1})]$ (<0.5 mM). The supporting electrolyte was 0.1 M tetrabutylammonium perchlorate. The applied potential was set beyond the $E^{0/}$ value of the first reduction potential, typically at -0.8 V versus the decamethylferrocene/decamethylferrocenium couple. For the transient resonance Raman measurements, the excitation source at 354.7 nm was provided by the third harmonic of an Nd:YAG laser (Continuum, Surelite I-10), giving a power output of 10 mJ per pulse. Spectra were analyzed using GRAMS AI (Galactic Industries).

III. Results and Discussion

A recent paper by Lundin et al.[25] reported the synthesis of **1** and **2** and their $[Cu(PPh_3)_2]^+$ and $[Re(CO)_3Cl]$ complexes studied in this work, along with the synthesis of $[Ru(bpy)_2]^{2+}$ complexes of the two ligands. The crystal structures of the $[Re(CO)_3Cl]$ complexes were reported and discussed. The paper also reported electronic absorption spectroscopy, fluorescence and lifetime studies of the compounds, and the electroluminescence properties of $[Re(CO)_3Cl(\mathbf{1})]$. DFT studies (B3LYP/6-31G-(d)) were used to calculate ground-state structures, which were compared with the reported crystal structures. The efficacy of calculated structures for which no crystal structures were available was tested by calculating vibrational spectra from these structures, which were compared with experimental IR and nonresonance Raman spectra. The preliminary DFT study in this earlier paper established that the mean absolute deviation between calculated and experimental band frequencies for the major bands within the ligand vibration region (1000−1650 cm^{-1}) was less than 6 cm^{-1} for complexes and ligands.

This work aims to better understand the structural changes attendant upon these complexes with photoexcitation; to accomplish this a number of different states were studied. The nonresonance Raman spectra and calculations on the compounds (Section III.a) can assist in interpretation of the nature of photoexcitation (the FC state). We have further probed the FC state by examining the resonance Raman spectra of the compounds (Section III.b). Analysis of these data in concert with DFT calculations provides insight into the nature of the absorbing chromophore. To study the thermally equilibrated excited (THEXI) state, we have measured the spectra of electrochemically reduced complexes, which may act as a model for ligand reduction present in MLCT excited states[29−33] (Section III.C). This analysis is assisted by DFT calculations on the reduced ligands and complexes. The THEXI states for the complexes are probed using transient resonance Raman spectroscopy (Section III.D). Calculations on the lowest-energy triplet state provide an interpretive guide to the transient resonance Raman data.

III.A. Ground State. The FC state is generated by optical excitation, and has the same nuclear coordinates as the ground state. Thus, the calculation of the ground state can be used to model the FC state.

Nonresonance Raman Spectra. The nonresonance Raman spectra of *fac*-$[Re(CO)_3Cl(\mathbf{1})]$ and *fac*-$[Re(CO)_3Cl(\mathbf{2})]$ have been reported previously to support the validity of calculated structures.[25]

The nonresonance Raman spectra of the ligands and complexes, collected using an FT-Raman system, are shown in Figure 2. The simulated spectra produced by calculations are presented in the Supporting Information, Figure A. The FT-Raman spectrum of **1** shows a number of bands that may be attributed to modes localized on different portions of the ligand structure, specifically, phen-based, phz-based, and delocalized modes.[33,34] The band observed (predicted) at 1031 cm^{-1} (1032 cm^{-1}) is a phenanthroline mode, involving motion of the A, B, and C rings. This is also the case for bands observed at 1323 cm^{-1} (1337 cm^{-1}) and 1587 cm^{-1} (1600 cm^{-1}) and a shoulder at 1598 cm^{-1} (1611 cm^{-1}). Delocalized modes are observed at 1469 cm^{-1} (1474 cm^{-1}) and 1532 cm^{-1} (1546 cm^{-1}). There are a number of phenazine-based vibrations at 1410 cm^{-1} (1403 cm^{-1}) and 1621 cm^{-1} (1632 cm^{-1}). The calculated modes correspond closely with modes predicted for the dppz ligand in

a previous study.[34] The mode assignments can be found in the Supporting Information, Table B.

Upon complexation to copper(I), there are a number of small shifts in these bands. The most significant difference is the increased intensity of the phen mode at 1437 cm^{-1} (1439 cm^{-1}). Complexation to rhenium(I) results in a differing intensity pattern and slight wavenumber shifts for modes at 1594 and 1606 cm^{-1}, which are phen modes observed at 1587 and 1598 cm^{-1} in the free ligand. A strong band appears at 1050 cm^{-1} and this band is characterized as a phen mode.

The FT-Raman spectrum of **2** is similar to that of **1**, with phen features at 1031 cm^{-1} (1031 cm^{-1}), 1327 cm^{-1} (1336 cm^{-1}) and 1587 cm^{-1} (1600 cm^{-1}). The shoulder at 1598 cm^{-1} is not evident. A strong phz band appears at 1402 cm^{-1} (1396 cm^{-1}) (Figure 2d); this corresponds to the 1410 cm^{-1} band in **1**. A delocalized mode appears at 1536 cm^{-1} (1542 cm^{-1}). Complexation of **2** to copper(I) and rhenium(I) centers produces small changes to the FT-Raman spectrum, similar to those observed for complexation of **1** to copper(I) and rhenium(I) centers (Figure 2e,f). Complexation to copper(I) causes increased intensity of modes at 1437 cm^{-1} (1437 cm^{-1}) and 1586 cm^{-1} (1594 cm^{-1}). *fac*-[$Re(CO)_3Cl$(**2**)] has a strong mode at 1052 cm^{-1} (1053 cm^{-1}) which is not observed in the FT-Raman spectrum of the free ligand or the copper(I) complex.

The ester carbonyl stretch for **1** in the solid state is measured at 1715 cm^{-1} (1751 cm^{-1}) (Figure 2a). The predicted frequency of this mode in $[Cu(PH_3)_2$(**1**)$]^+$ is 1759 cm^{-1}; this frequency upshift is in qualitative agreement with the experimental band which appears at 1717 cm^{-1} for $[Cu(PPh_3)_2$(**1**)$]^+$. For *fac*-[$Re(CO)_3Cl$(**1**)] the mode appears at 1707 cm^{-1} (1756 cm^{-1}). The experimental downshift is not qualitatively reproduced in the calculation. However, this vibrational mode for *fac*-[$Re(CO)_3Cl$(**1**)] has previously been reported at 1723 cm^{-1} in CH_3CN, and this result is in qualitative agreement with the calculated value.[22] The frequency for this mode in the free ligand was not reported by the authors. The observed frequency shifts upon complexation to the respective metal centers suggests that the metal center has an influence on the phz end of the ligand, which is likely to be exerted electronically through the extended π-system.

fac-[$Re(CO)_3Cl$(L)] complexes are useful in probing MLCT states because their carbonyl ligands are sensitive to the oxidation state of the rhenium center.[35,36] In the ground state, the three carbonyl modes have a_1 and *e* symmetry; thus, two of these modes are degenerate, owing to the pseudo-C_{3v} symmetry about the metal center.[37] Calculations on *fac*-[$Re(CO)_3Cl$(**1**)] and *fac*-[$Re(CO)_3Cl$(**2**)] predict the ancillary carbonyl ligand vibrational modes in both complexes to have frequencies at 1961, 1983, and 2052 cm^{-1}. The solid-state FT-Raman spectrum of *fac*-[$Re(CO)_3Cl$(**1**)] has three ancillary carbonyl ligand bands at 1884, 1927, and 2032 cm^{-1}. These bands appear at 1889, 1917, and 2025 cm^{-1} for *fac*-[$Re(CO)_3Cl$(dppz)] in a KBr disk.[38] The FT-Raman spectrum of *fac*-[$Re(CO)_3Cl$(**2**)] shows a broad band centered at 1904 cm^{-1} and a weak band at 2023 cm^{-1}. Despite the remoteness of the substituent from the metal center, these differences between *fac*-[$Re(CO)_3Cl$(**1**)] and *fac*-[$Re(CO)_3Cl$(**2**)] suggest a level of electronic communication across the entire system. The influence of the 11-substituent on the ancillary carbonyl ligand modes is not predicted by the calculation. However, an electronic communication effect is evident in the MOs of the two rhenium(I) complexes; many of which are delocalized across the entire complex. In particular, the HOMO-1 for both ligands, which in *fac*-[$Re(CO)_3Cl$(**2**)] is lowered in energy to become the HOMO-6, has more electron density on the ancillary carbonyl ligands than does the same MO in *fac*-[$Re(CO)_3Cl$(**1**)], in which it is the HOMO-7 (Figure 3). The delocalization of this MO extends over the rhenium(I) center, carbonyl ligands, the Cl atom and the entire ligand to the substituent.

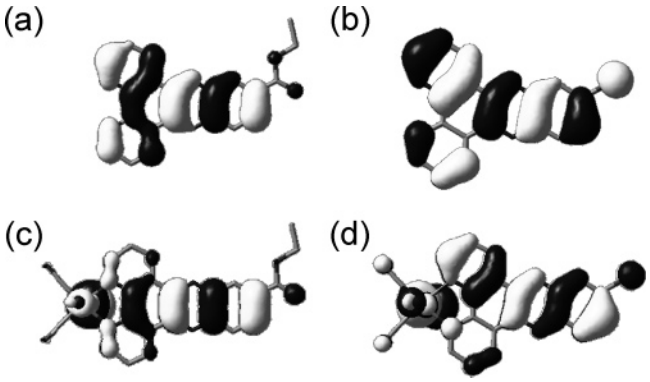

Figure 3. Molecular orbital diagrams of (a) **1** HOMO-1, (b) **2** HOMO-1, (c) *fac*-[$Re(CO)_3Cl$(**1**)] HOMO-7, and (d), *fac*-[$Re(CO)_3Cl$(**2**)] HOMO-6.

III.B. The Franck−Condon (FC) State. *Resonance Raman Spectra.* We have used resonance Raman spectroscopy to investigate the complex interplay of chromophores in the FC state. Resonance enhancement in these systems is confined to totally symmetric modes as their enhancement mechanism is through A-term scattering.[33] The strongest enhancement is seen in modes which have distortions that mimic those of the resonant transition from the ground to the FC state.[33,39] Therefore, it should be possible to ascertain the MO populated in the FC state from the pattern of band enhancements in the resonance Raman spectra. There are two types of transitions that can contribute to the absorption spectra in the low-energy region: these are the MLCT and LC transitions.[4] In the *fac*-[$Re(CO)_3Cl$(dppz)] complex, there is a prevalence of enhanced modes which are phen-based.[33] For this complex the FC state is Re $\rightarrow$ [b_1(phen)]. For the complex *fac*-[$Re(CO)_3$(py)(dppz)]$^+$, the "precursor" state formed is a LC state, possibly π-π^* (phen).[19]

The resonance Raman (RR) spectra for the ligands and complexes are presented in Figure 4. The RR spectra of the ligands provide a signature for their LC transitions. There are significant differences between the RR spectra of **1** and **2** (Figure 4). The mode at 1406 cm^{-1} in **1** is of lower relative intensity than the same mode (at 1399 cm^{-1}) in ligand **2**. This mode is the largest predicted band in the calculated FT-Raman spectrum for both ligands. The increased intensity of this phz mode in the RR spectrum of **2** relative to the RR spectrum of **1**, and the observation of another phz mode at about 1050 cm^{-1} in the RR spectrum of **2** and its complexes, which is not evident in the RR spectra of **1** and its complexes, suggests that phz modes are more prominent in **2**, and that the transition of this ligand which is resonant at 356 nm has more phz character. The LC transition of **1** appears to enhance phenanthroline or delocalized modes, although the strong mode at 1537 cm^{-1} is a phz mode.

The RR spectra of all four complexes show features at approximately 1316 cm^{-1}, 1350 cm^{-1}, 1406, 1450, and 1545 cm^{-1}. These bands are of similar frequency to those of the respective free ligands and have been observed in other dppz systems.[12,40,41] The mode assignments are shown in Table 1.

The RR spectra of complexes $[Cu(PPh_3)_2$(**1**)$]^+$ and *fac*-[$Re(CO)_3Cl$(**1**)] can be compared with that of **1** (λ_{exc} = 356 nm). If a similar intensity pattern is observed in the RR data of the complexes, this would indicate the FC state to be a LC state. The spectra of both complexes closely match that of the ligand. This suggests that the principal transition at 356 nm is LC in

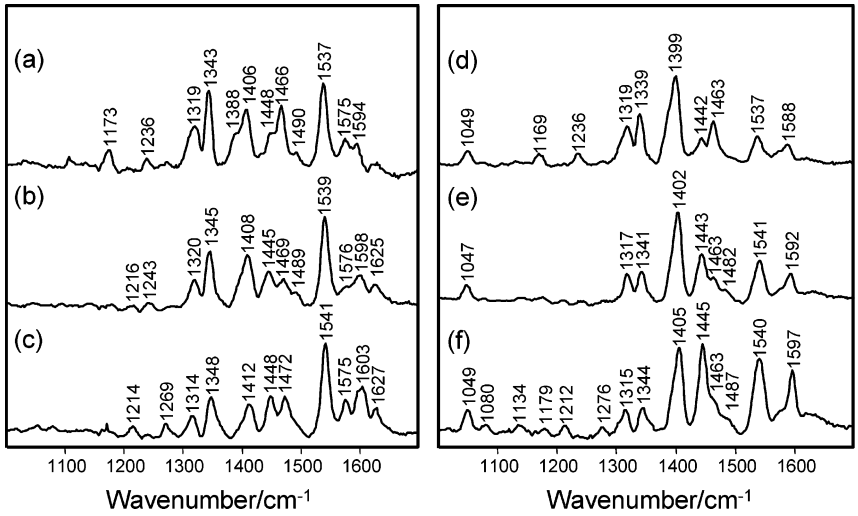

Figure 4. Resonance Raman spectra ($\lambda_{exc} = 356$ nm) (a) **1**, (b) $[Cu(PPh_3)_2(\mathbf{1})]^+$, (c) *fac*-$[Re(CO)_3Cl(\mathbf{1})]$, (d) **2**, (e) $[Cu(PPh_3)_2(\mathbf{2})]^+$, and (f) *fac*-$[Re(CO)_3Cl(\mathbf{2})]$. Solutions were prepared in $CDCl_3$ at concentrations of 0.5 mM.

TABLE 1: Band Assignments for Selected Vibrational Modes of Complexes Calculated at the B3LYP/6-31G(d) Level

	Assign ment for dppz	Assignment for substituted dppz ligands	Assignment for $Ru(phen)_2$ $dppz^{2+}$	Assignment from calculatio ns (this work)			
wavenum ber	ref 34	ref 32	ref 41	$[Cu(PH_3)_2(\mathbf{1})]^+$	$[Cu(PH_3)_2(\mathbf{2})]^+$	fac-$[Re(CO)_3Cl(\mathbf{1})]$	fac-$[Re(CO)_3Cl(\mathbf{2})]$
1316	Phen	phen		phz	phen	phz	phen
1350	phen		phz	phen	phz	phen	phz
1406	phz	delocalized	delocalized	phz	phz	phz	phz
1450	phen		phen	phen	delocalized	phen	delocalized
1545	phz			phz	phz	phz	phz

nature. There is a slight loss of enhancement of the delocalized 1466 cm^{-1} mode in the RR spectra of the $[Cu(PPh_3)_2(\mathbf{1})]^+$ and *fac*-$[Re(CO)_3Cl(\mathbf{1})]$ complexes, where the band shifts to 1469 and 1472 cm^{-1} respectively.

The RR spectra of 2, $[Cu(PPh_3)_2(\mathbf{2})]^+$, and *fac*-$[Re(CO)_3Cl(\mathbf{2})]$ are shown in Figure 4d−f. In this case, the spectra of the complexes are markedly different. The spectrum of $[Cu(PPh_3)_2(\mathbf{2})]^+$ is very similar to that of **2**, indicating that a LC chromophore in the complex dominates the absorption at 356 nm. The 1443 cm^{-1} phen band shows stronger enhancement, while the 1463 cm^{-1} phz band is diminished. However, the spectrum of *fac*-$[Re(CO)_3Cl(\mathbf{2})]$ shows significant spectral differences to that of **2**. Bands at 1445, 1540, and 1597 cm^{-1} show strong enhancement (Figure 5b) and are assigned by the calculation as delocalized, phz and phen modes, respectively. This shows that the FC state for *fac*-$[Re(CO)_3Cl(\mathbf{2})]$ is not like that of **2** and suggests the presence of at least one other chromophore, such as MLCT in which all sections of the ligand (both phen and phz) are involved, or a differing ^{1}LC transition. This is unsurprising, as near-UV excitation populates both ^{1}MLCT and ^{1}LC FC states in complexes of this nature.[19]

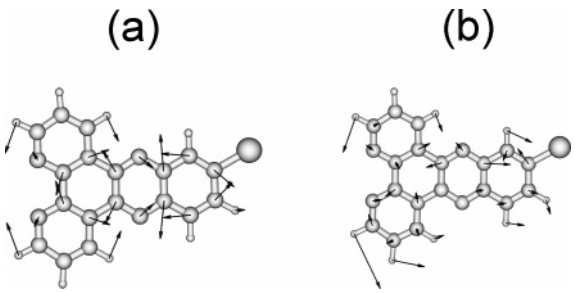

Figure 5. Selected vibrational modes of 2: (a) ν_{68}, calculated frequency 1396 cm^{-1}, observed frequency 1399 cm^{-1}, (b) ν_{71}, calculated frequency 1451 cm^{-1}, observed frequency 1442 cm^{-1}.

III.C. Model for the Lowest-Energy Triplet State. Resonance Raman Spectra of Reduced Complexes. The reduced species can be used as a model for the THEXI state.[29−33] The spectral signatures of $L^{\cdot-}$ may be obtained by taking the resonance Raman spectra of the electrochemically reduced metal complexes. These can then be compared with the transient resonance Raman spectra, to ascertain if there are $L^{\cdot-}$ spectral features or marker bands present, indicating an MLCT THEXI state.[33] The vibrational bands can shift in wavenumber depending on the nature of the redox MO;[33] if the reducing MO has bonding character across a certain bond, the wavenumber of normal modes associated with that bond will increase upon reduction.[42,43]

Coates et al. reported an excited-state resonance Raman feature at 1366 cm^{-1} for $[Ru(phen)_2dppz]^{2+*}$ and $[Ru(phen)_2(d_6\text{-dppz})]^{2+*}$ which is equivalent to the 1407 cm^{-1} band in the ground state.[41] It had been assigned as a phz mode.[40] From these studies it was concluded that the excited-state had $^3\pi$-π^* character. However, other studies suggeset that the downshift in frequency for this mode, with deuteration of the phen portion of the dppz, is consistent with a $dppz^{\cdot-}$ species, indicating that the excited state observed is MLCT in nature.[44] Identification of this band in the resonance Raman spectra of reduced *fac*-$[Re(CO)_3Cl(\mathbf{1})]^{\cdot-}$ and *fac*-$[Re(CO)_3Cl(\mathbf{2})]^{\cdot-}$ provides a marker for the radical anion of the ligand, which would be present in an MLCT state.

A phz ring stretch appears in the SCF lowest triplet state calculation of *fac*-$[Re(CO)_3Cl(\mathbf{1})]$ at 1371 cm^{-1} (ν_{104}). This mode appears in all calculations of the ligands and complexes, and has large eigenvectors across bonds r_9, r_{12}, and r_{14}/ $r_{14'}$. Figure 5a shows the eigenvectors of this mode for **2**. The calculated LUMO for **2** (Figure 6) is antibonding across these bonds, suggesting that population of the LUMO would have

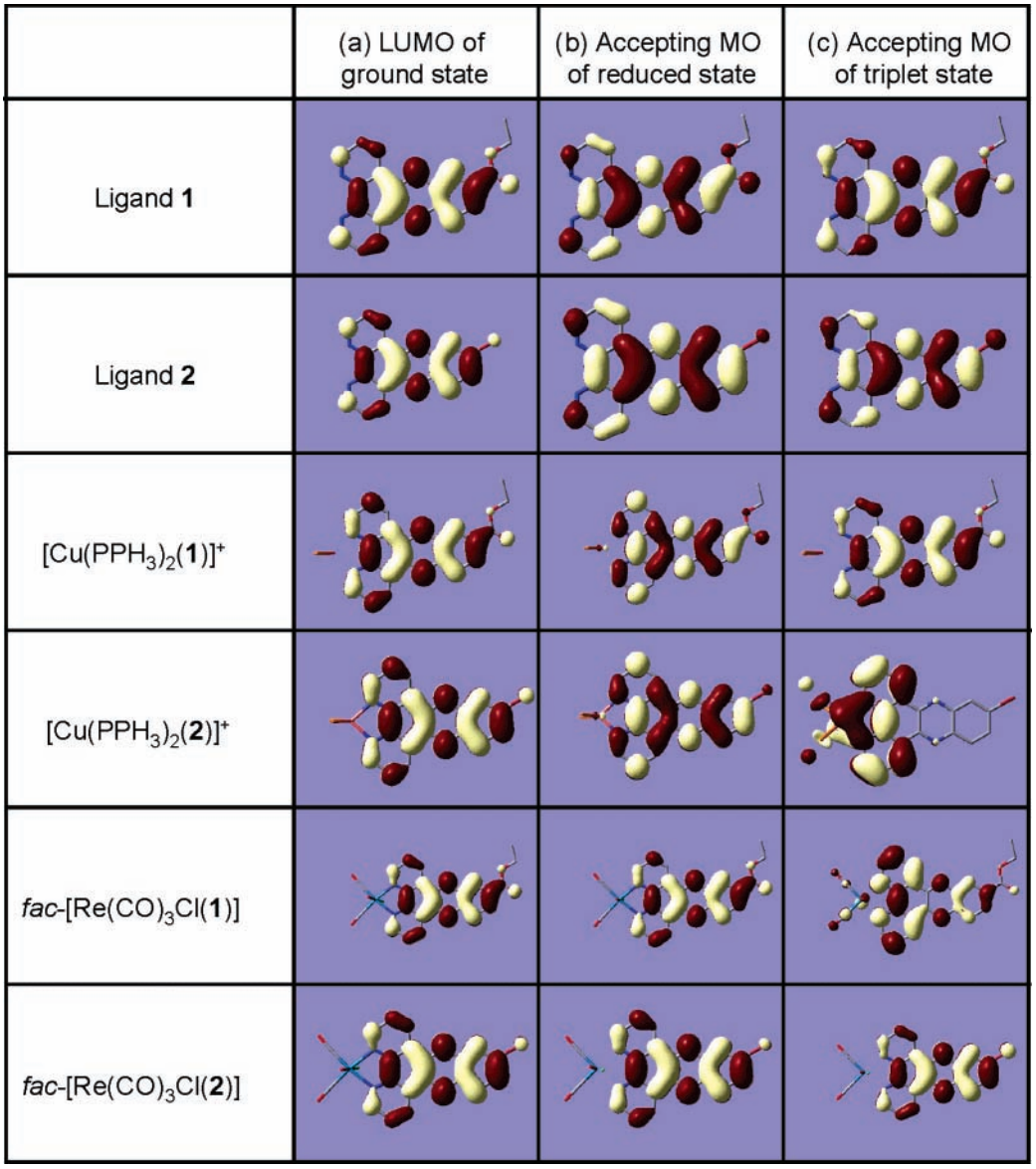

Figure 6. Molecular orbital diagrams for selected MOs of the compounds studied, calculated at the B3LYP/6-31G(d) level, (a) LUMO of ground state, (b) accepting MO of reduced state, and (c) accepting MO of triplet state.

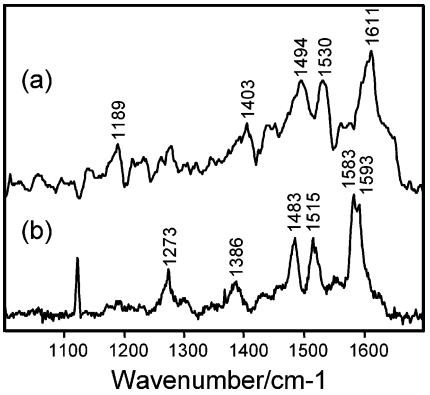

Figure 7. Resonance Raman spectra (λ_{exc} = 514.5 nm) of (a) *fac*-[Re(CO)$_3$Cl(**1**)]$^{\bullet-}$ and (b) *fac*-[Re(CO)$_3$Cl(**2**)]$^{\bullet-}$. Solutions were prepared in $CDCl_3$ at concentrations of 0.5 mM.

the effect of decreasing the frequency of the mode. This is also the case for **1** and the complexes.

The RR spectra of reduced complexes *fac*-[Re(CO)$_3$Cl(**1**)] and *fac*-[Re(CO)$_3$Cl(**2**)] (λ_{exc} = 514.5 nm) are shown in Figure 7. Excitation at 514.5 nm probes a visible absorption band of the reduced state, which is red-shifted from the ground-state absorption band.[33] The RR spectrum of *fac*-[Re(CO)$_3$Cl(**2**)]$^{\cdot-}$ has two strong bands at 1483 and 1515 cm^{-1}, and a broad band at 1583−1593 cm^{-1}. A feature at 1386 cm^{-1} may correspond to the 1405 cm^{-1} mode in the ground-state RR spectrum of *fac*-[Re(CO)$_3$Cl(**2**)]; this mode is observed at 1364 cm^{-1} [33] and 1357 cm^{-1} [34] in *fac*-[Re(CO)$_3$Cl(dppz)]$^{\cdot-}$. This pattern of bands is repeated in the Raman OTTLE spectrum of *fac*-[Re(CO)$_3$Cl(**1**)], suggesting that the accepting MOs for reduction are similar. However, in *fac*-[Re(CO)$_3$Cl(**1**)], the bands are slightly blue-shifted.

The Raman OTTLE spectrum of *fac*-[Re(CO)$_3$Cl(dppz)] shows bands at 1357 cm^{-1}, 1456, 1491, and 1580 cm^{-1}, and it was concluded that the reducing MO for this complex is phz-based.[34] Although this general pattern of bands is reproduced in the Raman OTTLE spectra of *fac*-[Re(CO)$_3$Cl(**1**)] and *fac*-[Re(CO)$_3$Cl(**2**)], the wavenumber-shifts of the bands suggest that either the reducing electron is occupying an entirely different MO for these complexes, or that the MO is only slightly different and the enhanced modes are shifted in frequency. For *fac*-[Re(CO)$_3$Cl(**2**)], the calculation on the reduced complex assigns the bands at 1483 cm^{-1}, 1515 cm^{-1} and 1583−1593 cm^{-1} as phen/delocalized, phz and phen modes,

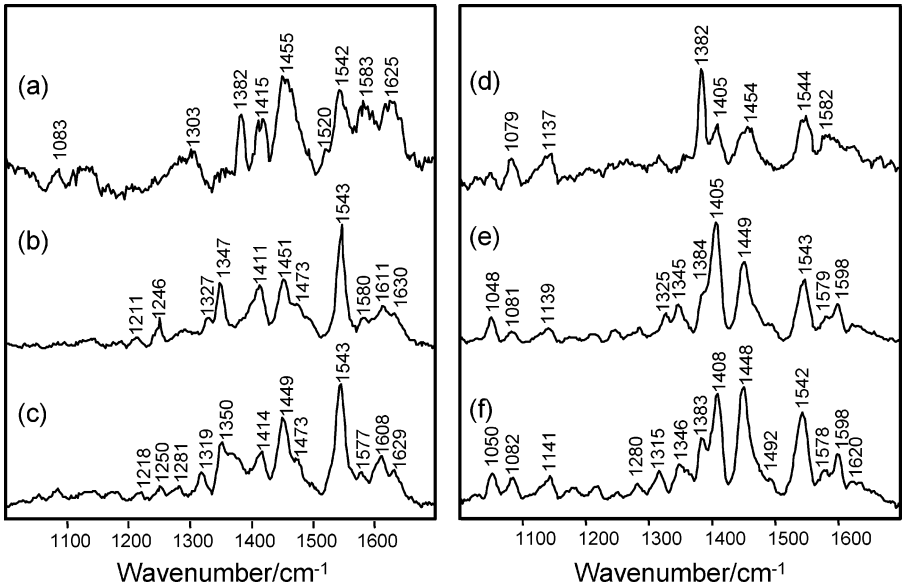

Figure 8. Transient resonance Raman spectra (λ_{exc} = 354.7 nm) of (a) **1***, (b) [Cu(PPh$_3$)$_2$(**1**)]$^{+*}$, (c) *fac*-[Re(CO)$_3$Cl(**1**)]*, (d) **2***, (e) [Cu(PPh$_3$)$_2$(**2**)]$^{+*}$, and (f) *fac*-[Re(CO)$_3$Cl(**2**)]*. Solutions were prepared in CDCl$_3$ at concentrations of 0.5 mM.

respectively. For reduced *fac*-[Re(CO)$_3$Cl(**1**)], they are assigned as ester/ delocalized, phz and delocalized modes, respectively. As the wave function for the singly occupied MO (SOMO) (Figure 6) for both reduced complexes has a similar appearance and is delocalized over the whole ligand, modes which are both phen, phz, and delocalized are enhanced. This suggests that the π* accepting MOs for the substituted ligands are more delocalized than for dppz, in agreement with the previous study.[25]

Calculated Geometry Changes upon Reduction. For both *fac*-[Re(CO)$_3$Cl(**1**)] and *fac*-[Re(CO)$_3$Cl(**2**)], the calculations predict the HOMO to be metal-based, and the LUMO ligand-based. Geometry changes on reduction of **1** and **2** are calculated to be localized on the phz portion of the ligand, suggesting that the reducing MO (SOMO) is the b$_1$(phz) MO. This is supported by electrochemical studies. The first reduction potential for complexes [Cu(PPh$_3$)$_2$(**1**)]$^+$ and [Cu(PPh$_3$)$_2$(**2**)]$^+$ are −0.85 and −0.95 V respectively, demonstrating that the first reduction potential for the complexes is affected by the substituent at the E-ring.[25] The LUMOs of **1** and **2** are shown in Figure 6. There is little electron density on the coordinated nitrogen atoms. In reduced **1** and **2**, these MOs are the accepting SOMOs.

The changes observed upon reduction of the ligand 1 (i.e. **1** → **1**$^{\bullet-}$) are similar to those seen when comparing [Cu(PH$_3$)$_2$(**1**)]$^+$ and [Cu(PH$_3$)$_2$(**1**)]$^\bullet$. The major geometry changes on reduction of [Cu(PH$_3$)$_2$(**1**)]$^+$ are on the phz portion of the ligand, extending out onto the ester. There are some additional perturbations to the phen portion; notably, r_5 is 1.7 pm shorter than $r_{5'}$. The calculations predict that the accepting SOMO for [Cu(PH$_3$)$_2$(**1**)]$^\bullet$ is a delocalized ligand MO (Figure 6). There are some changes about the copper center, notably shortening of Cu−N and lengthening of Cu−P bonds. The geometry changes on reduction of [Cu(PPh$_3$)$_2$(**2**)]$^+$ are similar to geometry changes of reduction of [Cu(PPh$_3$)$_2$(**1**)]$^+$ and are localized on the phz portion (see Supporting Information, Table C).

Geometry changes in fac-[Re(CO)$_3$Cl(**1**)] upon reduction are localized on the phz portion and ester substituent. Geometry changes about the metal center include a lengthening of the Re−Cl bond by 1.2 pm. Geometry changes in *fac*-[Re(CO)$_3$Cl(**2**)] on reduction are similar to those in *fac*-[Re(CO)$_3$Cl(**1**)], with a phz/Br localization and changes to the Re−Cl bond of 1.2 pm.

Spin Density Distribution upon Reduction. Mulliken spin density analysis gives an indication of the location of the reducing electron. Spin density distribution (SDD) of **1** and **2** show that electrochemical reduction would cause the reducing electron to be localized on the phz portion. The ester substituent in **1** distorts the electron localization asymmetrically. Atoms which in dppz are equivalent with respect to the C_2 axis are assigned differing or even opposite spins; for example, the two carbon atoms joined by bond r_9 are assigned −0.040 and +0.067 spin, respectively. While some of the spin is localized on the ester in **1**, the Br substituent in **2** has less of a distorting effect on the spin density.

The calculation on [Cu(PH$_3$)$_2$(**1**)]$^\bullet$ has a spin density distribution which is delocalized somewhat asymmetrically over the ligand. Spin density in the calculation on [Cu(PPh$_3$)$_2$(**2**)]$^\bullet$ is also quite delocalized over the ligand. There is no unpaired electron density on the copper(I) center in either case. *fac*-[Re(CO)$_3$Cl(**1**)]$^{\bullet-}$ has unpaired spin asymmetrically distributed over the phz portion. The calculation on *fac*-[Re(CO)$_3$Cl(**2**)]$^{\bullet-}$ shows unpaired spin delocalized over the ligand, but not the Br atom.

III.D. Lowest-Energy Triplet State. Transient Resonance Raman Spectra. The transient resonance Raman spectrum of **1*** measured with 354.7 nm excitation (Figure 8a) differs from the ground-state spectrum o**f 1** (Figure 4a). Most notably, the ground-state features at 1174 and 1343 cm^{-1} are absent in the transient spectrum. This suggests that the species probed in the transient spectrum includes no residual ground state. The TR^2 spectrum of 1 has strong features at 1382, 1455, and 1542 cm^{-1}. These bands are attributed to the LC THEXI state of the ligand, with the 1382 cm^{-1} band acting as a distinctive marker band.

The spectrum of [Cu(PPh$_3$)$_2$(1)]$^{+*}$ is quite different from that of **1***. This suggests that the THEXI state of [Cu(PPh$_3$)$_2$(**1**)]$^{+*}$ has little or none of the ^{3}LC state characteristic of **1***. The TR^2 spectrum of [Cu(PPh$_3$)$_2$(**1**)]$^{+*}$ (Figure 8b) also differs from the RR spectrum of [Cu(PPh$_3$)$_2$(**1**)]$^+$ (Figure 4b), with many of the bands displaying small but significant shifts in wavenumber. While the solvent bands are within 1 cm^{-1} of each other, serving as an internal standard, the 1599 cm^{-1} band shifts to 1611 cm^{-1}, the 1409 cm^{-1} band shifts to 1411 cm^{-1}, and the 1320 cm^{-1} band moves to 1327 cm^{-1}. Similar blue shifts of up to 5 cm^{-1} are evident in many of the bands. The 1216 cm^{-1} band red-shifts to 1211 cm^{-1}. This suggests that for [Cu(PPh$_3$)$_2$(**1**)]$^{+*}$, the THEXI state is structurally slightly different from the ground state. For [Cu(PPh$_3$)$_2$(**1**)]$^{+*}$, bands are shifted from the ground-

state spectrum to the transient spectrum, these include phz modes at 1320, 1408, and 1539 cm^{-1}, phen modes at 1599 and 1627 cm^{-1}, and delocalized modes at 1445 and 1469 cm^{-1}. The greatest shift is in the 1599 cm^{-1} phen mode, followed by 1320 cm^{-1} phz mode. A new band is observed at 1370 cm^{-1}. The triplet state calculation has two modes which could be assigned to this band, a phz mode and a delocalized mode.

Dyer et al.[19] showed that for the complex *fac*-$[Re(CO)_3(dppz)(py)]^+$, the 1316 cm^{-1} band is replaced by a 1280 cm^{-1} band in the excited state, and the 1406 cm^{-1} band is shifted to 1408 cm^{-1}. This is consistent with a $\pi \rightarrow \pi^*$(dppz) (phz) LC state.[12] There is no band at 1280 cm^{-1} in the ground-state spectrum of $[Cu(PPh_3)_2(\mathbf{1})]^+$, and the 1316 cm^{-1} band which was present in the ground-state spectrum of *fac*-$[Re(CO)_3(dppz)(py)]^+$ appears at 1320 cm^{-1} (Figure 4 (b)). In the TR^2 spectrum of $[Cu(PPh_3)_2(\mathbf{1})]^{+*}$, the 1320 cm^{-1} ground-state band is not evident and the 1408 cm^{-1} excited state *fac*-$[Re(CO)_3(dppz)(py)]^+$ band appears at 1413 cm^{-1}, showing a similar trend to that observed for the ^{3}LC state in *fac*-$[Re(CO)_3(dppz)(py)]^+$. However, this $^3\pi-\pi^*$ state in $[Cu(PPh_3)_2(\mathbf{1})]^{+*}$ differs from that of $\mathbf{1}^*$. This could be the reason for the slight spectral shifts observed. The presence of the $dppz^{\cdot -}$ band at 1580 cm^{-1} in the TR^2 spectrum of $[Cu(PPh_3)_2(\mathbf{1})]^{+*}$ indicates the presence of MLCT species in the THEXI state, although the band appears at 1611 cm^{-1} in the RR spectrum of the reduced complex. In any case this band is weak and suggests that the MLCT state is not the sole excited state observed in the TR^2 spectrum.

The ground-state RR spectrum of $[Cu(PPh_3)_2(\mathbf{2})]^+$ has a dominant band at 1403 cm^{-1} which appears at 1405 cm^{-1} in the TR^2 spectrum, while the ground-state band at 1318 cm^{-1} is shifted to 1325 cm^{-1}. These shifts are similar to those observed for $[Cu(PPh_3)_2(\mathbf{1})]^+$, showing that the THEXI states of $[Cu(PPh_3)_2(\mathbf{2})]^{+*}$ and $[Cu(PPh_3)_2(\mathbf{1})]^{+*}$ are similar. The TR^2 spectrum of $[Cu(PPh_3)_2(\mathbf{2})]^{+*}$ includes features seen in the TR^2 spectrum of $\mathbf{2}^*$ at 1081 and 1141 cm^{-1}, indicating the presence of two distinct ^{3}LC states. However, the 1383 cm^{-1} band seen in $\mathbf{2}^*$ is now only a shoulder and the 1407 and 1451 cm^{-1} bands dominate the spectrum.

A number of previous studies have provided marker bands for respective MLCT transitions, i.e., terminating on a phen or phz π^* ligand MO. Picosecond-transient resonance Raman studies on $[Ru(bpy)_2(dppz)]^{2+}$ identified a strong peak at 1361 $\pm$ 10 cm^{-1} in aqueous solution, which was assigned to a band solely associated with the excited state.[45] A similar band appears at 1390 cm^{-1} in acetonitrile.[45,46] It has been shown that there are two phases of decay following excitation of $[Ru(phen)_2dppz]^{2+}$, and that these modes are associated with the MLCT′ (Ru$\rightarrow b_1$(phen)) and MLCT″ (Ru$\rightarrow b_1$(phz)) states, respectively.[46] A strong feature at 1526 cm^{-1} had been identified as a marker band for a ^{3}MLCT state,[47] and this was attributed to the MLCT′ state.[46] Deuteration studies show that it is a phen-localized mode;[34] this is consistent with the MLCT″ state dominating in water. $dppz^{\cdot -}$ bands have been reported to occur at 1261, 1316, 1366, 1455, 1545, and 1575 cm^{-1}.[46,48]

The TR^2 spectrum of *fac*-$[Re(CO)_3Cl(\mathbf{1})]^*$ is very similar to that of $[Cu(PPh_3)_2(\mathbf{1})]^{+*}$. It shows growth of a broad feature over 1360−1380 cm^{-1} which is not present in the ground-state RR spectrum. This broad feature encompasses the marker band region at 1382−1386 cm^{-1}, and could be attributed to the ^{3}LC band at 1382 cm^{-1}, or the $L^{\cdot -}$ marker band at 1386 cm^{-1} observed in the Raman OTTLE spectrum. A new band at 1366 cm^{-1} is also present in this region; this 1366 cm^{-1} band is more pronounced in the TR^2 spectrum of *fac*-$[Re(CO)_3Cl(\mathbf{1})]^*$ in CH_2Cl_2 (not shown). Thus, the TR^2 spectrum of *fac*-$[Re(CO)_3Cl(\mathbf{1})]^*$ is consistent with the presence of an LC state similar to $[Cu(PPh_3)_2(\mathbf{1})]^{+*}$, which differs from that of $\mathbf{1}^*$. In addition the new broad feature at above 1350 cm^{-1} could indicate a $L^{\cdot -}$ species, or MLCT state. The 1580 cm^{-1} band is also present, indicating an MLCT state which is not the dominant species. Shifts of other bands, similar to those in $[Cu(PPh_3)_2(\mathbf{1})]^{+*}$, are less pronounced, but include 1604 to 1608 cm^{-1}, 1315 to 1319 cm^{-1}, and 1270 to 1281 cm^{-1}.

The TR^2 spectrum of $\mathbf{2}^*$ is very similar to that of $\mathbf{1}^*$, in contrast to the ground-state RR spectra. This suggests a THEXI state which is not affected by the substituent, i.e., $^3\pi$-π^* (phen). The band at 1383 cm^{-1} is more intense in the TR^2 spectrum of $\mathbf{2}^*$ (Figure 8d) than in that of $\mathbf{1}^*$.

The TR^2 spectra of $[Cu(PPh_3)_2(\mathbf{2})]^{+*}$ and *fac*-$[Re(CO)_3Cl(\mathbf{2})]^*$ are similar to each other but show significant differences from their respective ground states. The spectra of $[Cu(PPh_3)_2(\mathbf{2})]^{+*}$ and *fac*-$[Re(CO)_3Cl(\mathbf{2})]^*$ both show some intensity for the LC marker band at 1382 cm^{-1}. Excitation of *fac*-$[Re(CO)_3Cl(\mathbf{2})]^*$ at 354.7 nm results in a number of other spectral changes; most notably, the ground-state band at 1315 cm^{-1} shows diminished intensity, and a weak band at 1463 cm^{-1} in the ground state is bleached in the TR^2 spectrum. The 1382 cm^{-1} band and a weak band at 1360 cm^{-1} are not present in the ground state, and a number of the other bands show slight shifts to higher wavenumber; for example, 1405 cm^{-1} shifts to 1407 cm^{-1}. The 1080 and 1142 cm^{-1} ^{3}LC bands are also present. This suggests that the triplet state of $[Re(CO)_3Cl(\mathbf{2})]^*$ has both MLCT and LC character.

Calculated Structures. Calculated geometry changes on excitation of ligands **1** and **2** to the lowest triplet state are localized on the phz portion of the ligand. For **1** and **2**, large changes of 5−6 pm between the triplet and ground state are observed on the E-ring, with 2−5 pm changes on the C and D rings. There are virtually no changes on the A and B rings, or on the ester group of **1**.

$[Cu(PPh_3)_2(\mathbf{1})]^+$ has similar behavior to the free ligand, in that the predicted geometry changes are on the phz portion upon excitation to the lowest triplet state. Nonetheless, there are significant differences between the geometries of the respective triplet excited states of **1** and $[Cu(PPh_3)_2(\mathbf{1})]^+$. These differences are at the E-ring and ester group. The calculations predict that an electron will occupy a delocalized ligand MO. In the triplet state, the excited electron is located in a phz-based ligand-centered MO and the vacated π-MO is also on the phz portion. This is indicative of a LC state. Thus, the calculation on $[Cu(PH_3)_2(\mathbf{1})]^{+*}$ predicts an LC state which is structurally different from the LC state of the ligand. This is in agreement with the TR^2 findings, which do not show the aforementioned MLCT bands, but show LC bands for $[Cu(PPh_3)_2(\mathbf{1})]^{+*}$ which differ from that of $\mathbf{1}^*$.

The triplet state of *fac*-$[Re(CO)_3Cl(\mathbf{1})]$ is strikingly different from that of $[Cu(PH_3)_2(\mathbf{1})]^+$. The principal structural changes on going to the triplet state from the ground state are on the A and B ring systems. There are only very small ($|\Delta r| < 1$ pm) structural changes at the E ring system. On excitation of *fac*-$[Re(CO)_3Cl(\mathbf{1})]$, the geometry changes are localized on the phen portion. Re−N bonds decrease by 3 and 9 pm, the Re−Cl bond decreases by 10 pm, and Re−C bonds lengthen by 5−6 pm. There are also small decreases in C−O bond length. The HOMO of *fac*-$[Re(CO)_3Cl(\mathbf{1})]$ is metal-centered, and the LUMO is a delocalized ligand-centered MO. The accepting MO in the triplet state calculation has phen character (Figure 6).

In the triplet excited state of $[Cu(PH_3)_2(\mathbf{2})]^+$, geometry changes are predicted to be localized on the phen region. The

accepting SOMO in the triplet state (b_1(phen)) differs from that of $[Cu(PH_3)_2(\mathbf{1})]^+$ (Figure 6). This has a significant effect on the calculated geometry around the copper center, with Cu−N bonds shortened significantly and Cu−P bonds lengthened. The PH_3 ligands are displaced, with the dihedral angle P−Cu−N−C being reduced from 65° to 33°. Similar geometric distortions have been suggested for many copper(I) diimine complexes.[49]

Geometry changes of *fac*-[Re(CO)$_3$Cl(**2**)] on excitation are localized on the phz portion, with some small perturbations on the phen portion of the ligand. The Re center undergoes some distortion: one of the Re−N bonds shortens by 1.5 pm while the other remains constant. The Re−C_{eq} bond trans to this bond is lengthened by 1.6 pm.

Spin Density Distribution and MOs upon Excitation. Excitation to the lowest triplet state results in two electrons of unpaired spin. Unpaired spin on the metal center is indicative of an MLCT state. The reorganization of the electrons can have an effect on the shape and energy of the MOs.

Triplet excitation of **1** and **2** leads to the formation of a ligand-centered $\pi-\pi^*$ state. In these states the excited electron occupies an MO which is phz-based and the unpaired spins are localized on that section of the respective ligands. The triplet states of the metal complexes may be LC or MLCT in character. Furthermore, the acceptor MO in the MLCT states may be a phz-, phen- or delocalized ligand MO. In the series studied, a number of differing CT states are predicted. The spin density distribution and accepting MO in the triplet state of $[Cu(PH_3)_2(\mathbf{1})]^+$ are strikingly similar to those of the free ligand (Figure 6). The metal center possesses no unpaired spin, suggesting a LC state. In the lowest triplet state of $[Cu(PH_3)_2(\mathbf{2})]^+$, the acceptor MO is consistent with an MLCT state in which the ligand π^* MO is phen-based (Figure 6): 0.88 spin is located on the copper center and PH_3 ligands, and 1.12 spin is located on the phen portion. However, the corresponding complex *fac*-[Re(CO)$_3$Cl(**2**)] has an MLCT state in which the excited electron terminates on a phz-based MO (Figure 6): in the triplet state, 1.42 spin is located on the phz portion and Br substituent and 0.31 spin on the Re moiety. The triplet state of complex *fac*-[Re(CO)$_3$Cl(**1**)] has 0.92 unpaired spin on the phen portion, with 0.166 extending to the phz region and 0.93 spin about the Re center and ancillary ligands. For this complex, the excited electron vacates a metal-centered MO, to terminate on a phen-based ligand-centered MO (Figure 6).

IV. Conclusions

We have established the nature of FC and THEXI states for a number of complexes with substituted dppz ligands. The ground states of these complexes have been shown to be susceptible to electronic modulation by substitution. Resonance Raman spectroscopy shows that for ligand **2**, the FC state has more phz character than for ligand **1**. The FC states of complexes of **1** are LC states. For $[Cu(PPh_3)_2(\mathbf{2})]^+$, the FC state is a LC in nature similar to that of **2**, but for *fac*-[Re(CO)$_3$Cl(**2**)], the FC state has some MLCT character involving a delocalized ligand MO.

The studies on the electrochemically reduced complexes show that the MO populated by reduction of *fac*-[Re(CO)$_3$Cl(**1**)] and *fac*-[Re(CO)$_3$Cl(**2**)] is phz-based, but has a more delocalized character than that of dppz. TR^2 experiments identified a marker band for the ^{3}LC state of both ligands at 1382 cm^{-1}. TR^2 spectra of the complexes show both ^{3}LC and ^{3}MLCT features, indicating the presence of both of these states.

The triplet calculations suggest that the THEXI state is ^{3}LC (phz) for ligands **1** and **2**, and for $[Cu(PH_3)_2(\mathbf{1})]^+$; MLCT (phen) for complexes $[Cu(PH_3)_2(\mathbf{2})]^+$ and *fac*-[Re(CO)$_3$Cl(**1**)] and MLCT (phz) for *fac*-[Re(CO)$_3$Cl(**2**)]. Experimentally, it was found that the major THEXI state was a similar ^{3}LC state for **1** and **2**. For $[Cu(PPh_3)_2(\mathbf{1})]^{+*}$ the THEXI state is an LC state which differs from that of $\mathbf{1}^*$; there is also a little MLCT character similar to the $L^{\bullet-}$ species generated by electrochemical reduction. The THEXI state of $[Cu(PPh_3)_2(\mathbf{2})]^{+*}$ comprises several different configurations. It has some of the LC character of the free ligand and also some differing LC character, similar to the $[Cu(PPh_3)_2(\mathbf{1})]^{+*}$ complex. Some MLCT character is also present to a small degree. The THEXI state of *fac*-[Re(CO)$_3$Cl(**1**)]* contains a mixture of the LC state found for $[Cu(PPh_3)_2(\mathbf{1})]^{+*}$ and a ^{3}MLCT state indicated by dppz$^{\bullet-}$ bands at 1251 and 1366 cm^{-1} in the transient resonance Raman spectrum. Similarly, *fac*-[Re(CO)$_3$Cl(**2**)]* appears to have a THEXI state comprising of contributions from a $[Cu(PPh_3)_2(\mathbf{2})]^{+*}$-like LC configuration, a $\mathbf{2}^*$-like LC configuration and an MLCT configuration indicated by the 1611 cm^{-1} band. The calculation only identifies the lowest-energy triplet state so perhaps for these systems TDDFT is more appropriate. TDDFT calculations will be attempted and may help to identify the energetic ordering of these differing states; however, time-dependent modeling of these systems is difficult and results should be interpreted with caution.

Supporting Information Available: Simulated ground-state FT-Raman spectra (Figure A), mode assignments for ground states of ligands and complexes (Table B), calculated geometry changes upon reduction, and triplet excitation of ligands and complexes (Table C) are available free of charge via the Internet at http://pubs.acs.org. This material is contained in libraries on microfiche, immediately follows this article in the microfilm version of the journal, and can be ordered from the ACS; see any current masthead page for ordering information.

References and Notes

(1) Coates, C. G.; Jacquet, L.; McGarvey, J. J.; Bell, S. E.; Al-Obaidi, A. H. R.; Kelly, J. M. *Chem. Commun.* **1996**, 35.

(2) Broo, A.; Lincoln, P. *Inorg. Chem.* **1997**, *36*, 2544.

(3) Coates, C. G.; McGarvey, J. J.; Callaghan, P. L.; Coletti, M.; Hamilton, J. G. *J. Phys. Chem. B* **2001**, *105*, 730.

(4) Stoeffler, H. D.; Thornton, N. B.; Temkin, S. L.; Schanze, K. S. *J. Am. Chem. Soc.* **1995**, *117*, 7119.

(5) Schoonover, J. R.; Bates, W. D.; Meyer, T. J. *Inorg. Chem.* **1995**, *34*, 6421.

(6) Olson, E. J. C.; Hu, D.; Hormann, A.; Jonkman, A. M.; Arkin, M. R.; Stemp, E. D. A.; Barton, J. K.; Barbara, P. F. *J. Am. Chem. Soc.* **1997**, *119*, 11458.

(7) Schoonover, J. R.; Strouse, G. F.; Dyer, R. B.; Bates, W. D.; Chen, P.; Meyer, T. J. *Inorg. Chem.* **1996**, *35*, 273.

(8) Brennaman, M. K.; Alstrum-Acevedo, J. H.; Fleming, C. N.; Jang, P.; J. Meyer, T.; Papanikolas, J. M. *J. Am. Chem. Soc.* **2002**, *124*, 15094.

(9) Dattelbaum, D. M.; Omberg, K. M.; Hay, P. J.; Gebhart, N. L.; Martin, R. L.; Schoonover, J. R.; Meyer, T. J. *J. Phys. Chem. A* **2004**, *108*, 3527.

(10) Amouyal, E.; Homsi, A.; Chambron, J. C.; Sauvage, J. P. *J. Chem. Soc., Dalton Trans.* **1990**, 1841.

(11) Schoonover, J. R.; Bignozzi, C. A.; Meyer, T. J. *Coord. Chem. Rev.* **1997**, *165*, 239.

(12) Waterland, M. R.; Gordon, K. C.; McGarvey, J. J.; Jayaweera, P. M. *J. Chem. Soc., Dalton Trans.* **1998**, 609.

(13) Kalyanasundaram, K.; Gratzel, M. *Coord. Chem. Rev.* **1998**, *177*, 347.

(14) Navarro, M.; Cisneros-Fajardo Efren, J.; Sierralta, A.; Fernandez-Mestre, M.; Silva, P.; Arrieche, D.; Marchan, E. *J. Biol. Inorg. Chem.* **2003**, *8*, 401.

(15) Delaney, S.; Pascaly, M.; Bhattacharya Pratip, K.; Han, K.; Barton Jacqueline, K. *Inorg. Chem.* **2002**, *41*, 1966.

(16) David, G.; Walsh, P. J.; Gordon, K. C. *Chem. Phys. Lett.* **2004**, *383*, 292.

(17) Pourtois, G.; Beljonne, D.; Moucheron, C.; Schumm, S.; Kirsch-De Mesmaeker, A.; Lazzaroni, R.; Bredas, J.-L. *J. Am. Chem. Soc.* **2004**, *126*, 683.

(18) Fantacci, S.; De Angelis, F.; Sgamellotti, A.; Re, N. *Chem. Phys. Lett.* **2004**, *396*, 43.

(19) Dyer, J.; Blau, W. J.; Coates, C. G.; Creely, C. M.; Gavey, J. D.; George, M. W.; Grills, D. C.; Hudson, S.; Kelly, J. M.; Matousek, P.; McGarvey, J. J.; McMaster, J.; Parker, A. W.; Towrie, M.; Weinstein, J. A. *Photochem. Photobiol. Sci.* **2003**, *2*, 542.

(20) Batista, E. R.; Martin, R. L. *J. Phys. Chem. A* **2005**, *109*, 3128.

(21) George, M. W.; Turner, J. J. *Coord. Chem. Rev.* **1998**, *177*, 201.

(22) Kuimova, M. K.; Grills, D. C.; Matousek, P.; Parker, A. W.; Sun, X.-Z.; Towrie, M.; George, M. W. *Vib. Spectrosc.* **2004**, *35*, 219.

(23) Adamson, A. W. *J. Chem. Educ.* **1983**, *60*, 797.

(24) Dattelbaum, D. M.; Omberg, K. M.; Schoonover, J. R.; Martin, R. L.; Meyer, T. J. *Inorg. Chem.* **2002**, *41*, 6071.

(25) Lundin, N. J.; Walsh, P. J.; Howell, S. L.; McGarvey, J. J.; Blackman, A. G.; Gordon, K. C. *Inorg. Chem.* **2005**, *44*, 3551.

(26) Frisch, M. J.; G. W. T.; Schlegel, H. B.; Scuseria, G. E.; Robb, M. A.; Cheeseman, J. R.; Montgomery, Jr., J. A.; Vreven, T.; Kudin, K. N.; Burant, J. C.; Millam, J. M.; Iyengar, S. S.; Tomasi, J.; Barone, V.; Mennucci, B.; Cossi, M.; Scalmani, G.; Rega, N.; Petersson, G. A.; H. N.; Hada, M.; Ehara, M.; Toyota, K.; Fukuda, R.; Hasegawa, J.; Ishida, M.; Nakajima, T.; Honda, Y.; Kitao, O.; Nakai, H.; Klene, M.; Li, X.; Knox, J. E.; Hratchian, H. P.; Cross, J. B.; Adamo, C.; Jaramillo, J.; Gomperts, R.; Stratmann, R. E.; Yazyev, O.; Austin, A. J.; Cammi, R.; Pomelli, C.; Ochterski, J. W.; Ayala, P. Y.; Morokuma, K.; Voth, G. A.; Salvador, P.; Dannenberg, J. J.; Zakrzewski, V. G.; Dapprich, S.; Daniels, A. D.; Strain, M. C.; Farkas, O.; Malick, D. K.; Rabuck, A. D.; Raghavachari, K.; Foresman, J. B.; Ortiz, J. V.; Cui, Q.; Baboul, A. G.; Clifford, S.; Cioslowski, J.; Stefanov, B. B.; Liu, G.; Liashenko, A.; Piskorz, P.; Komaromi, I.; Martin, R. L.; Fox, D. J.; Keith, T.; Al-Laham, M. A.; Peng, C. Y.; Nanayakkara, A.; Challacombe, M.; Gill, P. M. W.; Johnson, B.; W. C.; Wong, M. W.; Gonzalez, C.; Pople, J. A. *Gaussian 03*; Gaussian, Inc.: Pittsburgh, PA, 2003.

(27) Howell, S. L.; Gordon, K. C. *J. Phys. Chem. A* **2004**, *108*, 2536.

(28) Schaftenaar, G.; Noordik, J. H. *J. Comput. Aided Mol. Des.* **2000**, *14*, 123.

(29) Bignozzi, C. A.; Argazzi, R.; Schoonover, J. R.; Gordon, K. C.; Dyer, R. B.; Scandola, F. *Inorg. Chem.* **1992**, *31*, 5260.

(30) McGarvey, J. J.; Bell, S. E. J.; Gordon, K. C. *Inorg. Chem.* **1988**, *27*, 4003.

(31) Gordon, K. C.; McGarvey, J. J. *Inorg. Chem.* **1991**, *30*, 2986.

(32) Waterland, M. R.; Simpson, T. J.; Gordon, K. C.; Burrell, A. K. *J. Chem. Soc., Dalton Trans.* **1998**, 185.

(33) Waterland, M. R.; Gordon, K. C. *J. Raman Spectrosc.* **2000**, *31*, 243.

(34) Matthewson, B. J.; Flood, A.; Polson, M. I. J.; Armstrong, C.; Phillips, D. L.; Gordon, K. C. *Bull. Chem. Soc. Jpn.* **2002**, *75*, 933.

(35) Chen, P.; Palmer, R. A.; Meyer, T. J. *J. Phys. Chem. A* **1998**, *102*, 3042.

(36) Omberg, K. M.; Schoonover, J. R.; Meyer, T. J. *J. Phys. Chem. A* **1997**, *101*, 9531.

(37) Cotton, F. A.; Kraihanzel, C. S. *J. Am. Chem. Soc.* **1962**, *84*, 4432.

(38) Waterland, M. R. Spectroelectrochemistry and time-resolved spectroscopy of some copper(I) and rhenium(I) complexes in solution. Ph.D. Thesis, University of Otago, Dunedin, New Zealand, 1998.

(39) Hirakawa, A. Y.; Tsuboi, M. *Science* **1975**, *188*, 359.

(40) Chen, W.; Turro, C.; Friedman, L. A.; Barton, J. K.; Turro, N. J. *J. Phys. Chem. B* **1997**, *101*, 6995.

(41) Coates, C. G.; Callaghan, P. L.; McGarvey, J. J.; Kelly, J. M.; Kruger, P. E.; Higgins, M. E. *J. Raman Spectrosc.* **2000**, *31*, 283.

(42) McNicholl, R.-A.; McGarvey, J. J.; Al-Obaidi, A. H. R.; Bell, S. E. J.; Jayaweera, P. M.; Coates, C. G. *J. Phys. Chem.* **1995**, *99*, 12268.

(43) Schoonover, J. R.; Chen, P.; Bates, W. D.; Dyer, R. B.; Meyer, T. J. *Inorg. Chem.* **1994**, *33*, 793.

(44) Chen, W.; Turro, C.; Friedman, L. A.; Barton, J. K.; Turro, N. J. *J. Phys. Chem. B* **1998**, *102*, 6303.

(45) Benniston, A. C.; Matousek, P.; Parker, A. W. *J. Raman Spectrosc.* **2000**, *31*, 503.

(46) Coates, C. G.; Olofsson, J.; Coletti, M.; McGarvey, J. J.; Oenfelt, B.; Lincoln, P.; Norden, B.; Tuite, E.; Matousek, P.; Parker, A. W. *J. Phys. Chem. B* **2001**, *105*, 12653.

(47) Coates, C. G.; Jacquet, L.; McGarvey, J. J.; Bell, S. E. J.; Al-Obaidi, A. H. R.; Kelly, J. M. *J. Am. Chem. Soc.* **1997**, *119*, 7130.

(48) Coates, C. G.; Callaghan, P.; McGarvey, J. J.; Kelly, J. M.; Jacquet, L.; Kirsch-De Mesmaeker, A. *J. Mol. Struct.* **2001**, *598*, 15.

(49) Elder, R. C.; Lunte, C. E.; Rahman, A. F. M. M.; Kirchhoff, J. R.; Dewald, H. D.; Heineman, W. R. *J. Electroanal. Chem. Inter. Electrochem.* **1988**, *240*, 361.